Infratentorial Morphometry and Deep Brain Stimulation Outcome in Cervical Dystonia

Luke Andrews BSc, MSc* [1,2], Simon S. Keller BSc, MSc, PhD [1], Jibril Osman-Farah MD, MRCS, FRCS [2], Maneesh Bhojak MBBS, FRCR [2], Antonella Macerollo MD, PhD, MRCP [1,2]

[1] The Department of Pharmacology and Therapeutics, Institute of Systems, Molecular and Integrative Biology, University of Liverpool, UK; [2] The Walton Centre NHS Foundation Trust, Liverpool, UK

Abstract

Background: Cervical dystonia is a movement disorder, characterised by involuntary head and neck muscle contractions. Although deep brain stimulation (DBS) of the globus pallidus internus (GPi) is an effective treatment option, motor outcomes can vary even when sufficient targeting accuracy is achieved. Increasing evidence supports a role of brainstem and cerebellum dysfunction in cervical dystonia pathogenesis.

Objective: To determine whether morphometry of brainstem and dentate nuclei, and DBS stimulatory overlap with cerebello-thalamic tracts modelled from normative connectivity, were related to DBS clinical motor outcomes.

Methods: 27 patients with idiopathic cervical dystonia underwent bilateral targeting of the GPi. and were separated into suboptimal and optimal motor outcome groups. Dentate nuclei and brainstem volumes were quantified in association with clinical outcomes. A brainstem shape analysis was conducted and used as a seed to assess connectivity from a normative structural connectome. Patient-specific electrodes were modelled to quantify stimulatory overlap with the GPi and proximity to cerebellothalamic tracts.

Results: GPi implantation accuracy did not significantly differ between groups. Significantly reduced dentate nuclei and brainstem volumes were observed in patients with poorer clinical outcomes. Regional surface shape change of the brainstem was also observed in patients with poorer responses. Fibre tracking from this area intersected cerebellar, pallidal and cortical motor regions. Electrode field intersection with the non-decussating dentatorubrothalamic tract in the right, and in both hemispheres were also positively associated with clinical outcome.

Conclusions: Variability in cerebellar and brainstem morphometry, and stimulation of non-decussating cerebello-thalamic pathways may contribute to the mediation of DBS motor outcomes.

Introduction

Cervical dystonia is an isolated focal movement disorder that causes involuntary muscular contractions of the neck, resulting in pain, cramping and abnormal posturing.(1) Deep brain stimulation (DBS) of the globus pallidus internus (GPi) has proven to be an effective therapeutic option for the treatment of medically refractory cervical dystonia.(2,3) Whilst the accuracy of GPi targeting in dystonia is the best predictor for a favourable outcome from DBS, in some cases, sufficient motor symptom improvements may still not be achieved.(4–6) The partial predictive ability of implantation accuracy and the poor understanding of disorder aetiology warrants the need for additional explanatory biomarkers for cervical dystonia. Identifying patients who have increased likelihoods of greater outcomes is paramount to reliably inform patient selection.

Once thought to be a sole disorder of the basal ganglia, research has elucidated dystonia to reflect a "circuitopathy", indicating aberrant networks underpinning the pathophysiology.(7,8) Lesion-identification studies have identified spinal cord, basal ganglia, brainstem, cerebellum, and thalamic regions as most affected in patients with cervical dystonia,(9,10) with the brainstem and cerebellum as the most commonly affected regions in a recent study.(11) All lesion sites have been classified to ascertain connectivity with the cerebellum,(10) and surmounting evidence supports cerebellar involvement in dystonic sensorimotor pathophysiology.(7,8,12–14)

Brain-based imaging markers offer a potential avenue to explore variability in patients with cervical dystonia, in relation to therapeutic DBS outcomes. For example, functional MRI-derived connectivity has identified increased GPi-cerebellum and GPi-somatomotor cortex associations as indicative of greater and poorer clinical outcomes, respectively.(10) Furthermore, recent work using functional and tractography-derived connectivity identified the same network pattern, encapsulating the cerebellum and somatosensory cortex, as "optimal" pathways for therapeutic DBS outcomes in patients with cervical dystonia.(15)

Assessing the structure of the cerebellum and brainstem through imaging offers an alternative approach to explore these insights in relation to DBS outcomes. Cortico-ponto-cerebellar and cerebello-thalamo-cortical tracts form the structural connections that interlink the cerebellum, brainstem, regions of the basal ganglia and sensorimotor cortices.(16–19) Evidence of brainstem and cerebellar structural abnormalities have been observed in patients with cervical dystonia relative to healthy controls.(20–23) Pre-operative brain volumes have been seldom explored for DBS efficacy in cervical dystonia. To date, one study observed increased cerebellar vermis grey volume to be associated with improved outcomes.(24) To the best of our knowledge, no research has assessed brainstem structure in relation to DBS outcomes in cervical dystonia.

Assessment of white matter tracts offer an additional approach to assess brain structure in relation to DBS outcomes. The dentatorubrothalamic tract (DRTT) is a tract that has gained increasing popularity for importance of DBS outcomes in movement disorders including Parkinson's disease and essential tremor,(25–28) but has yet to be explored in cervical dystonia. Originating at the dentate nucleus of the cerebellum, classically defined decussating and more recently disclosed non-decussating tracts, convey cerebellar output to the thalamus, with onward projections to sensorimotor cortex.(29–31) Evidence for structural changes in cerebello-thalamo-cortical and specific DRTT pathways have been identified in DYT1/DYT6 and cervical dystonia, respectively.(32,33) Probing this pathway in the context of DBS modulation could present as a powerful biomarker for cervical dystonia pathophysiology, aiding patient selection and treatment prediction.

The present study aimed to address these questions by quantifying brainstem volume and brainstem shape morphometry to determine relationships with clinical DBS motor improvements. We hypothesised that patients with poorer motor outcomes would have volumetric reductions in comparison to patients with improved responses. In a subsequent analysis using a structural normative connectome, we sought to determine whether connectivity from brainstem areas found to be different between outcome groups would map to subcortical and cortical sensorimotor regions. In doing so, areas of change may occupy networks involved in cervical dystonia pathophysiology and aid potential therapeutic DBS mediation. Finally, we explored the role of the decussating and non-decussating DRTT's by first quantifying volumes of cerebellar dentate nuclei (as the DRTT origination point) and then assessing the relationship between stimulation fields and active contact proximities relative to the tracts in relation to motor improvements. We hypothesised that patients with poorer motor outcomes from DBS would have reduced dentate nuclei volumes and that electric field overlap coverage and contact proximity would be greater and closer to both DRTT pathways, respectively.

Methods

Patient Cohort

A retrospective cohort of 27 patients diagnosed with idiopathic cervical dystonia and treated with bilateral DBS was recruited from the movement disorders clinics at the Walton Centre NHS Foundation Trust (Liverpool, UK). Inclusion criteria included no structural lesions identifiable on the diagnostic MRI protocol, including pre-operative 2D T2, 2D T2-FLAIR and 3D T1-weighted magnetic resonance imaging (MRI), a confirmatory post-operative CT scan and available pre-and-post-operative clinical motor scores.

The Toronto Western Spasmodic Torticollis Rating Scale (TWSTRS) was carried out by a neurologist to measure cervical dystonia motor symptoms pre-and-post DBS implantation.(34) The TWSTRS score (T_{out}) was used as the outcome variable in the current study and was calculated using the following formula: $T_{out} = \frac{(T_{pre} - T_{post})}{T_{post}} * 100$ The T_{out} for each patient was obtained at the best improvement score between three and five years post-DBS implantation to provide a long-term clinically stabilised score,(35–37) excluding two patients who due to the recency of date of implantation, best two-year post-operative scores were used. Unlike movement disorders such as Parkinson's disease, at shorter time periods, the response of dystonia to DBS is not stable, suggested to be related to motor-plasticity effects from pallidal DBS.(38) To create groups based on motor response to DBS, patients were assigned to a sub-optimal response group given a T_{out} of < 66% and an optimal-response group given a T_{out} of ≥ 66%.

DBS Implantation

All patients included in the current study underwent DBS surgery at the Walton Centre NHS Foundation Trust (Liverpool, UK) over a period of 11 years (2009 - 2020). Patients were implanted with bilateral leads in the GPi, excluding one patient who was implanted with bilateral leads targeting the ventral intermediate nucleus/zona incerta (VIM/ZI) for cervical dystonia and additional dystonic tremor. Different electrode models were implanted across the patient cohort, namely Medtronic 3387 (n = 5), St Judes Active Tip 6142/6145 (n = 17), Boston Scientific Vercise Directed (n = 3) and St Judes Directed 6172 (n = 1).

MRI Acquisition

3 Tesla 3D T1-weighted images were acquired across three different scanners. Acquisition using a Phillips Achieva system with an 8-channel SENSE head coil (Philips Medical Systems, Best, The Netherlands), of 1 mm^3 isotropic MPRAGE (gadolinium contrast enhancement (CE) in 10 patients and no CE in five patients), 256 slices (for 14 patients) and 288 slices (for one patient) flip angle of 8°, TE = 0.004, TR = 0.009. For the GE Discovery MR750 system (GE healthcare, USA) with a 16-channel head coil, isotropic 1 mm^3 in 1 patient and 1.4 mm^3 in 1 patient CE-SPGR with 256 slices, flip angle of 12°, TE = .003, TR = .008. For the Siemens MAGNETOM Skyra (Siemens, Healthineers, Germany) with a 20-channel head coil, 256 slices at a resolution of 1 mm x 1 mm x 0.9 mm CE-SPGR, with a flip angle of 9°, TE = .003, TR = .011.

Image Processing

An overview of the image processing pipeline is presented schematically in figure 1 and is described in detail in the following sections. As some images were acquired with contrast, all T1-weighted MRI were processed with SynthSR (https://github.com/BBillot/SynthSR), a convolutional neural network used to balance contrast and provide a T1-weighted 1mm isotropic MPRAGE image for each patient.(39) Synthesis of the images was a necessary step in the pipeline to improve grey and white matter contrast (and subsequent segmentation) of the original images and provide cross-scanner harmonisation. A post-operative computed tomography (CT) image was also obtained for each patient following DBS implantation.

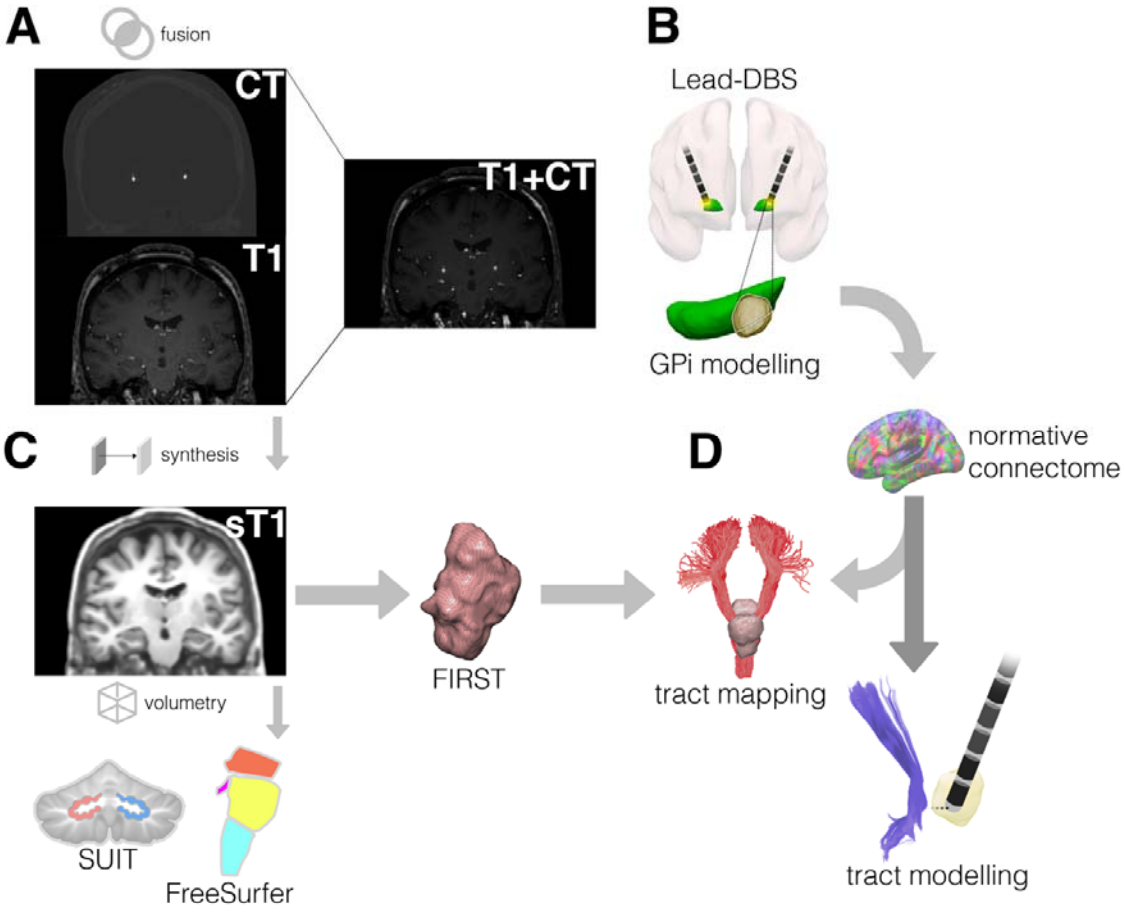

Figure 1. A) CT and T1-weighted MRI are fused. B) GPi stimulation overlap modelling performed within Lead-DBS. C) T1-weighted MRI are synthesised. Volumetric quantification of dentate nuclei is performed using SUIT and brainstem nuclei using FreeSurfer. FSL FIRST is used to calculate the brainstem shape analysis.D) A normative structural connectome is used to model tracts intersecting the brainstem shape analysis result. Additonally, electrodes are modelled in relation to cerebella-thalamic-tracts. Abbreviations: computed tomography, CT; dentatorubrothalamic tract, DRTT; FreeSurfer, FS; globus pallidus internus, GPi; Spatially Unbiased Infratentorial Template, SUIT; synthesised T1, sT1

Brainstem and Cerebellar Morphometry

To obtain volumetric estimates of the brainstem, the synthesised images were processed using FreeSurfer (version 7.2.0, https://surfer.nmr.mgh.harvard.edu). Bayesian segmentation was performed

in FreeSurfer to obtain grey matter volumes (mm^3) for pons, superior cerebellar peduncle (SCP), medulla, midbrain, and total brainstem.(40) The Spatially Unbiased Infratentorial Toolbox (SUIT; version 3.4, https://github.com/jdiedrichsen/suit/) was used to calculate grey matter volumes (mm^3) of left and right dentate nuclei of the cerebellum.(41) SUIT was used to first isolate the cerebellum from the rest of the brain using the synthesised T1-weighted MRI. Diffeomorphic anatomical registration through exponentiated lie algebra (DARTEL) was used to normalise the isolated cerebellar images into Montreal Neurological Institute (MNI) space.(42)

Brainstem Shape Analysis

To measure localised points of surface change of the brainstem, we used FSL-integrated registration and segmentation toolbox (FSL-FIRST; version 5.0; https://fsl.fmrib.ox.ac.uk/fsl/fslwiki/FIRST).(43) The brainstem was automatically segmented from the synthesised T1-weighted MRI images and vertex-wise comparisons were computed along the surface of the brainstem in MNI space. The contrast was focused on assessing where vertex-wise reductions may occur with regards to sub-optimal responders relative to optimal responders.

Electrode Modelling

Lead-DBS (version 2.6, https://www.lead-dbs.org) was used to model electrode trajectories for each patient.(44–46) 25 patients were included in lead modelling, with one patient being excluded due to poor CT acquisition and one patient being excluded due to implantation of the VIM/ZI for additional dystonic tremor. First, a two-stage linear co-registration of pre-operative MRI to post-operative CT was performed using advanced normalisation tools (ANTs; https://stnava.github.io/ANTs/).(47) Following this, ANTs SyN Diffeomorphic Mapping was used to normalise volumes to ICBM 2009b nonlinear asymmetric (“MNI”) space.(48) Brain shift correction was performed using a coarse mask. Electrode trajectories were pre-reconstructed for each patient manually within Lead-DBS and were inspected and refined by a movement disorder specialist. Patient-specific volume of tissue activated (VTA) were constructed using the FieldTrip-SimBio pipeline.(46)

DBS Analyses

To visualise the structural connectivity from the area of brainstem change, the FSL FIRST shape analysis mask was used to seed connectivity in the lead connectome mapper within Lead-DBS. The normative structural connectome MGH-USC HCP-32 was used to obtain a whole-brain fibre density map at a 0.5 mm resolution that permitted the analysis of the number of fibres connecting the brainstem ROI to all other voxels.(49)

The VTA-GPi overlap was calculated to assess implantation accuracy in the cohort. The DISTAL atlas was used to calculate overlap with the whole GPi, and the sensorimotor (posteroventral) region.(50) Here, one patient was removed due to targeting of the VIM/ZI for additional dystonic tremor (n = 25).

To assess the relationship between DBS and the cerebellar tracts, electric field distribution and contact proximity approaches were used. Three patients were excluded due to implantation of directional electrodes. Tract ROIs were obtained from the DBS tractography atlas.(51) Electric field distribution overlap was correlated with T_{out} scores for the left and right decussating and non-decussating DRTT's. To assess electrode proximity to these tracts, active contact positions for each electrode (left and right) were correlated in relation to the distance (mm) from these tracts with T_{out} scores. For each patient, the distance was averaged across active contacts for each electrode.

Statistics

Brainstem and dentate nuclei volumes were corrected for age, sex, and estimated total intracranial volume (eTIV; estimated from FreeSurfer) using the residuals from linear regression.(52) Volumes were compared between sub-optimal and optimal groups using two-sample t-tests. Statistical thresholds were Bonferroni corrected for the number of multiple comparisons. Corrections for cerebellar hemispheres ($p < 0.025$) and the four segmented brainstem nuclei ($p < 0.0125$) were performed.

Brainstem surface change was computed based on differences between the sub-optimal and optimal groups. The Threshold-Free Cluster Enhancement (TFCE) test-statistic was applied in randomise with 1000 permutations to identify clusters of voxels showing significant differences between groups. A threshold of $p < .05$ was used to as the level of significance. Age and sex were used as confounds in the model.

For Lead-DBS-based analysis, statistics were computed using Lead-group.(53) Linear regressions were used to assess the statistical significance of the VTA intersection with the GPi with a

threshold of p < .025 to correct for laterality and the electric field overlap and electrode proximity to pre-defined tracts with a corrected threshold of $p < 0.0125$.

Results

Patient Characteristics

For the surface and volumetric analyses, a total of 13 subjects were identified as optimal responders (six female) with 14 subjects identified as suboptimal responders (nine female). Optimal and sub-optimal responders did not show significant differences between age, eTIV or known disease duration ($p \geq .2$). The demographic information for this cohort is presented in table 1.

Table 1. Patient demographics

Age range (years)	Sex	Disease duration (years)	Pre-op TWSTRS	Post-op TWSTRS	T_{out}
65-70	F	26	46	36	21.7
35-40	F	20	64	40.5	36.7
60-65	M	6	61	48.25	20.9
45-50	F	19	45	40	11.1
60-65	M	7	56	6	89.3
35-40	M	25	69	18.75	72.8
70-75	F	11	36	6	83.3
55-60	F	8	52	40	23.1
65-70	F	10	57.75	44.75	22.2
45-50	M	11	53	15.75	70.3
55-60	F	11	47.25	32.25	31.7

60-65	M	3	40	26.5	33.8
40-45	M	12	35	14.25	59.3
60-65	F	18	48.5	10	79.4
65-70	F	26	30	35	-16.7
50-55	F	23	49	11	77.6
50-55	M	28	48.5	11.75	75.8
50-55	F	4	43.5	14	67.8
50-55	M	13	62	32	48.4
50-55	M	23	55.25	4	92.8
50-55	F	21	41	3.5	75.6
50-55	F	23	46	1	97.8
50-55	M	5	63	73.25	-16.3
20-25	F	10	30	20	33.3
50-55	M	4	45.75	14.25	68.9
50-55	F	2	61.75	44.5	27.9
50-55	F	14	60	13.25	77.9
M: 54.1 ± 10.6		M: 14.2 ± 8.2			M: 50.6 ± 32.3

Note. Demographic information of the cervical dystonia patient cohort in the present study. Patient ages are presented in ranges to anonymise identifiable information. Column mean ± standard deviation is presented in the bottom row. Abbreviations: mean, M; total outcome score, T_{out}; Toronto Western Spasmodic Torticollis Rating Scale, TWSTRS

Brainstem and Cerebellar Morphometry

Grey matter brainstem volumetry revealed significant differences in pons (t = 2.87, *p* = .009) and total brainstem (t = 2.73, *p* = .01) volume between outcome groups. SCP volume did not reach statistical significance following the correction for multiple comparisons (t = 2.26, *p* = .03). Medulla and midbrain volume differences did not reach statistical significance (t = 1.88, p = .07 and t = 1.78, p = .08, respectively). Left (t = -2.73, *p* = .0119) and right (t = -2.85, *p* = .008) dentate nuclei volumes were significantly different between groups. Results are presented in figure 2.

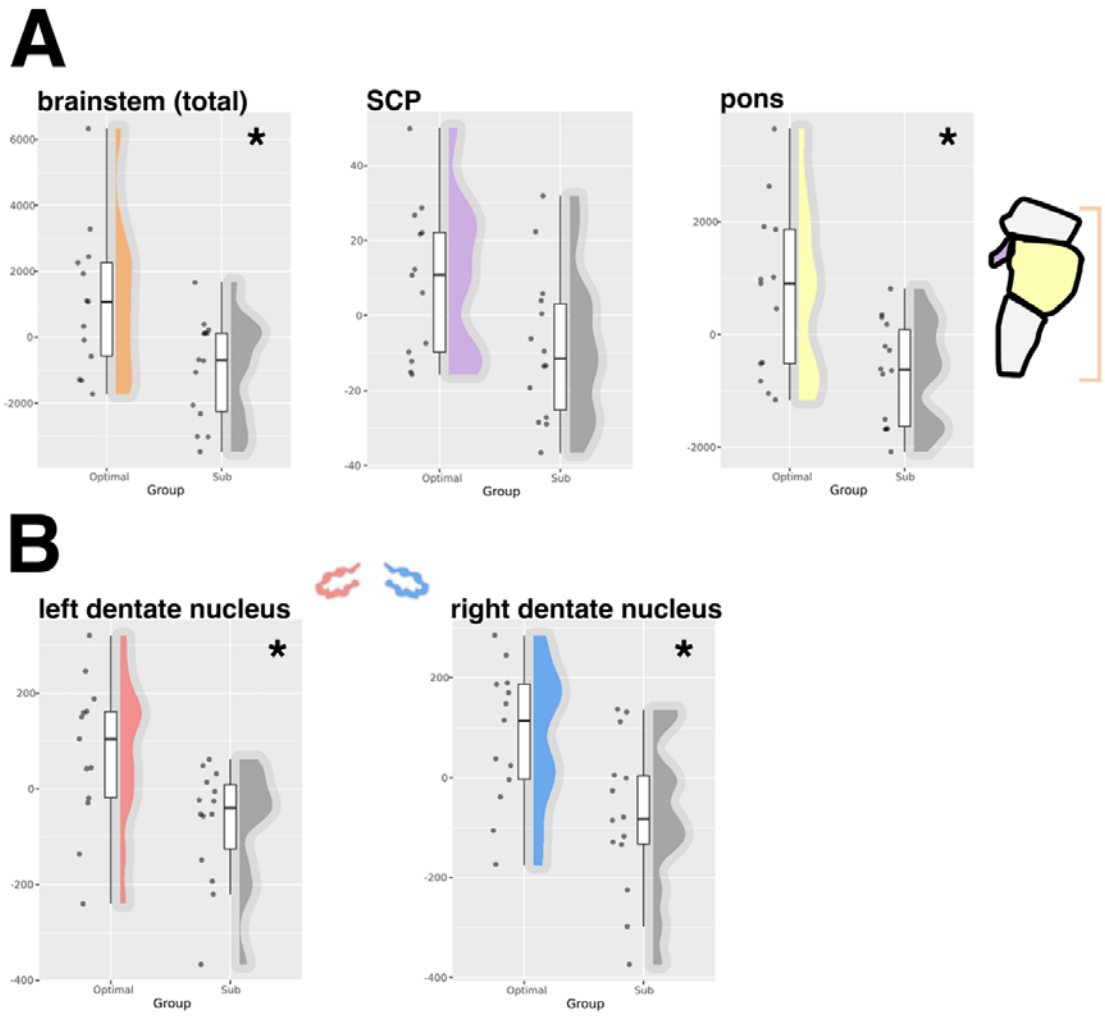

Figure 2. A) group comparisons of grey matter volume from FreeSurfer brainstem regions. B) group comparisons of dentate nuclei grey matter volumes from SUIT. * Indicates statistical significance following correction for multiple comparisons. Abbreviations: superior cerebellar peduncle; SCP

From the vertex-wise shape analysis, an area of left and right superior ventral and dorsal brainstem at the level of midbrain and pons showed inwards deflation in patients with a sub-optimal response, relative to an optimal response (figure 3A).

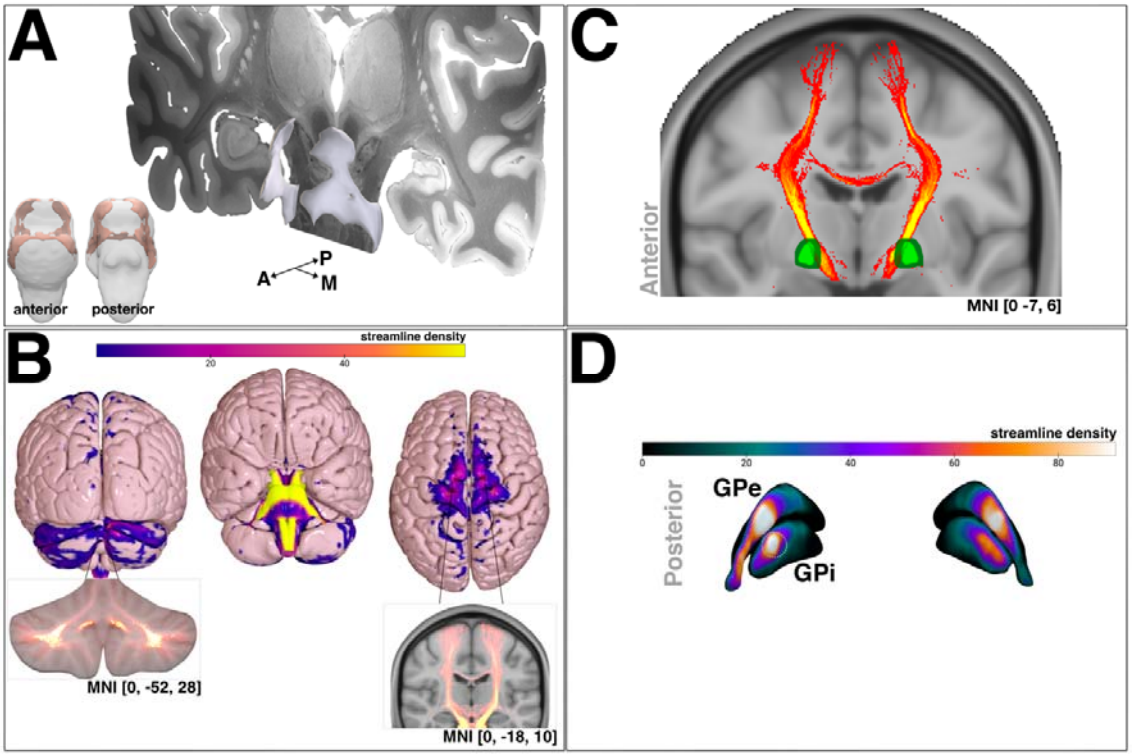

Figure 3. A) FSL FIRST brainstem shape analysis area showing inwards deflation between optimal and sub-optimal response groups (overlaid on the 7-tesla Ex Vivo 100µm Brain Atlas(54)). B) projected streamline density map showing cerebellar (left) and cortical motor (right) area termination. C) streamline density intersection of bilateral pallidum (masks obtained from the DISTAL atlas).(50) D) streamline density projection onto bilateral GPi/GPe renderings. The green circle overlaid on right GPi indicates the posteroventral region. Abbreviations: anterior, A; globus pallidus externus, GPe; globus pallidus internus, GPi; posterior, P; medial, M

Brainstem Connectivity Mapping

Normative connectivity was seeded from the brainstem area showing localised deflation in patients with sub-optimal responses (figure 3A) to create a whole-brain fibre density map. The fibre

density map reflects the streamline count and outlined termination at the cerebellum with intersection of the deep cerebellar nuclei and crus lobules I and II and VIIb (SUIT atlas; figure 3B, left)(41). Termination was also observed at cortical motor regions, particularly at medial premotor cortex, delineating 100% probability of intersection using the Juelich Histological Atlas, distributed with FSL (http://www.fmrib.ox.ac.uk/fsl/; figure 3B, right). Subcortically, intersection with the left and right pallidum at 100% probability was observed using the Harvard-Oxford Subcortical Structural Atlas, also distributed with FSL (figure 3C), and primarily traversed the posteroventral GPi (figure 3D).

Electrode Modelling, VTA Overlap and Tract Analysis

The placement of electrodes for the patient cohort is presented in figure 4A, showing optimal (n = 13) and sub-optimal (n = 12) responders.

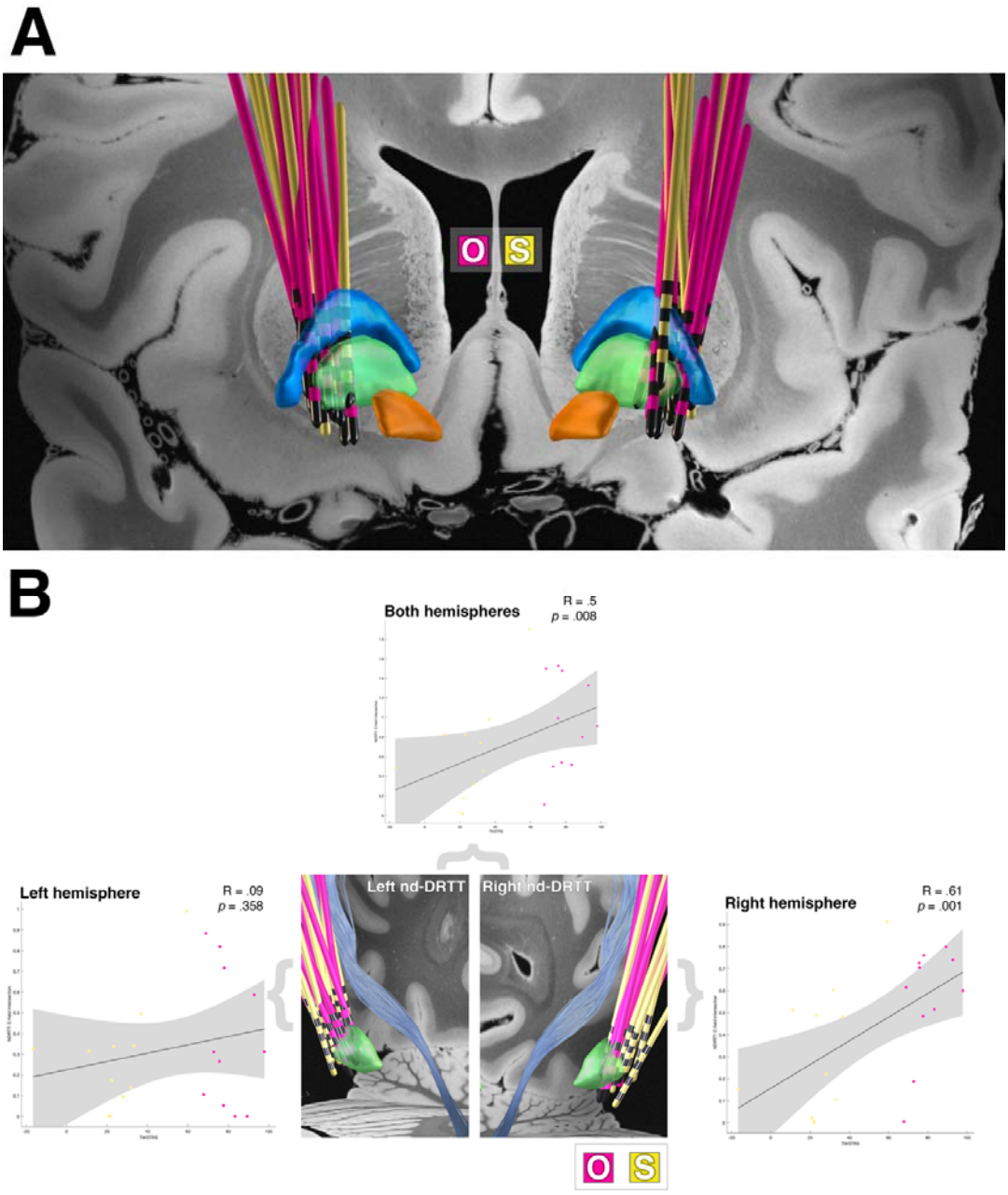

Figure 4. A) the lead placement of the patient cohort (overlaid on the 7-tesla Ex Vivo 100µm Brain Atlas(54)). The external pallidum (blue), internal pallidum (green) and subthalamic nucleus (orange) are visualised. B) correlations of normalised electric field intersection with the left and right non-decussating DRTT in relation to clinical outcome scores. Note, optimal responders are represented by the pink electrodes and sub-optimal responders by the yellow electrodes. Abbreviations: dentatorubrothalamic tract, DRTT; O, optimal responder leads; S, suboptimal responder leads

To test for lead placement between response groups, the normalised GPi-VTA overlap was computed for each patient. No significant association with clinical outcome was observed for VTA overlap with the whole GPi (R = .27, p = .09) or sensorimotor (posteroventral) GPi (R = .28, p = .09).

Normalised electric field intersections identified a significant positive relationship of overlap with the non-decussating DRTT on the right side (R = .61, p = .001) and with both hemispheres (R = .5, p = .008) with clinical outcome (figure 4B). The decussating tracts showed no significant associations with clinical outcome. When assessing the relationship between active contact proximity to the non-decussating DRTT (suboptimal: right (M: 9.4 ± 2.9 mm), left (M: 11.2 ± 2.7 mm); optimal: right (M: 8.7 ± 2.1 mm), left (M: 9.9 ± 2.4 mm)) and decussating DRTT (suboptimal: right (M: 7.4 ± 2.7 mm), left (M: 8.4 ± 2.2 mm); optimal: right (M: 6.9 ± 2.2 mm), left (M: 7.4 ± 2.3 mm)), no significant relations with T_{out} were observed for either tract (p > .4), nor were there any differences between groups.

Discussion

In the present study, we identified structural correlates related to the post-operative clinical motor outcome from DBS in patients with cervical dystonia. First, volumetric reduction of left and right dentate nuclei of the cerebellum and brainstem nuclei were observed in patients who experienced sub-optimal alleviation of motor symptoms from DBS treatment at long-term time-points (≥ 2-years) post-implantation. In addition, we report surface level changes, namely regional inward deflation of the brainstem, in the sub-optimal response group relative to the optimal response group. When normative structural connectivity was mapped from the surface area showing inwards deflation, probabilistic streamlines connected with cerebellar, subcortical and cortical motor regions, which corroborate a literature-defined network in cervical dystonia.(10,15) Analysis of electric field overlap with cerebellar tracts revealed that the non-decussating DRTT was significantly correlated with clinical outcome. Importantly, differences in clinical outcomes between patient groups appeared to not be driven by the accuracy of electrode placement, further enforcing the need to identify biomarkers beyond surgical accuracy. Taken together, our findings indicate potential new pathophysiological biomarkers for cervical dystonia that may aid in the identification of patients more likely to respond to DBS.

Volumetric reduction of the total brainstem, pons, and SCP (uncorrected) in patients with sub-optimal motor outcomes correspond to literature findings of affected areas in patients with cervical dystonia relative to healthy controls.(22,23) Pons and SCP connectivity, inferred using diffusion tractography, has previously been reported to show altered microstructural integrity, relative to

healthy controls.(20,21) Both the pons and SCP share connectivity with the cerebellum, through the cortico-ponto- and cerebello-thalamo-cortical pathways, respectively,(55,56) and are thus heavily involved in the neuroanatomical substrate of whole-brain motor pathways. The pons has been identified as an area associated with increased regional cerebral blood flow in patients with clinical improvements of cervical dystonia symptoms from GPi-DBS.(57) Furthermore, using functional MRI, increased activation of the pons accompanied by decreased activation of the sensorimotor cortex have been observed in patients with cervical dystonia when switching from optimal to non-optimal GPi-DBS settings.(58) Damage to the cerebellopontine angle, referring to the space between the pons and cerebellum, has been shown to elicit cervical dystonia in a single case study,(59) indicating a pathophysiological role of brainstem-cerebellar coupling in symptom generation.

Structural brain changes in focal dystonia are favoured within a compensatory framework in contrast to neurodegeneration.(60) Physiological cerebellar changes in focal dystonia have been debated to arise as part of the core pathology or as compensatory changes to basal ganglia dysfunction.(61,62) Purkinje cell loss, as observed in post-mortem patients with cervical dystonia,(12) is consistent with reduced cerebellar volumes identified in patients with poorer motor response to DBS. Purkinje cell loss has been proposed to result in diminished GABAergic olivo-cerebellar output to the thalamus,(63) resulting in greater impairment of motor networks, and in the current study, reduced efficacy of therapeutic targeting. In patients with cervical dystonia, reduced levels of GABA have been identified in the thalamus relative to healthy controls, supporting a hypothesis of deficient cerebellar outflow.(64) In rodent models, pharmacological dampening of purkinje cell spiking has been shown to elicit dystonic symptoms directly.(65) Furthermore, optogenetic dentate nucleus stimulation to dampen cerebello-thalamic excitability has been shown to directly reduce dystonic motor symptoms.(66)

Forming a structural pathway between the cerebellum, subcortical regions, and areas of the cortex, the DRTT poses as a novel therapeutic target for movement disorder DBS.(67) To the best of our knowledge, the DRTT in cervical dystonia has been explored in one previous study, showing altered markers of microstructure relative to healthy controls.(33) Namely, reduced fractional anisotropy of the left DRTT and reduced axial and mean diffusivity of the right DRTT were observed. Work addressing the non-decussating pathway was not identified. The strong associations of electric field overlap with the non-decussating DRTT in the current study present interesting findings in the context of DBS response. Aside from an evolutionary mechanism of ipsilateral cerebellar hemispheric capacity for bilateral motor control, diffusion tractography has shown that the decussating and non-decussating DRTT's project onto anatomically distinct thalamic regions. Non-decussating tracts favour targeting of ventroposterior thalamic nuclei whereas decussating tracts favour targeting of ventrolateral thalamic nuclei.(31) The ventroposterior nuclear complex has affiliation with somatosensory functioning, connecting with cortical sensorimotor regions.(68,69) It could be

theorised that modulating non-decussating DRTT could elicit corrective effects on abnormal cerebellar outflow with consequent upstream normalisation of aberrant sensorimotor processing.(70–72) The lack of significance for the left non-decussating DRTT is a novel finding and may be related to the dominant side of symptomology present in the patient cohort. However, as this data was not available in the current study, this question could not be explored further.

The observed connectivity pattern derived from the morphometric brainstem surface change supports a potential role of outcome mediation in a network-based manner. Intersection of the cerebellum and pallidum verifies lesion sites identified in patients with secondary cervical dystonia.(9–11) Posteroventral GPi intersection supports the brainstems involvement in mediating therapeutic networks, given that this area of the pallidum is widely regarded as the DBS hotspot for cervical dystonia, and occupies somatotopic cervical territory.(15,73,74) The observed cortical motor fibre intersection corroborates the somatotopic head and neck areas, as the terminus of white matter tracts associated with optimal clinical motor symptom reduction, in cervical dystonia.(15) Structural changes to primary and pre-motor regions,(22,75–77) and decreased resting-state functional MRI activity between cerebellar and primary motor cortex,(78) have been identified in patients with cervical dystonia relative to healthy controls, supporting a role of motor circuit changes in the disorder's pathophysiology.

Limitations

We acknowledge the limitations in the present study. Firstly, the use of SynthSR as a valid contrast balancing tool has yet to be independently validated. It is unclear how much variability is introduced in the image following synthesis; however, its application has shown reliable volumetric estimations from anisotropic 2D images, which are less desirable than the 3D isotropic images used in the present study. (Iglesias et al, 2021) Also, due to scans being acquired across three separate scanners, systematic variability in volumetric estimates cannot be ruled out entirely. SynthSR was favoured for both these cases by first, providing a degree of harmonisation across scanners, and second, showing high visual consistency pre-and-post synthesis following manual inspection.

The restriction to T1-weighted images due to the routine clinical care MRI protocol was a limitation in this study. The addition of 3D T2 and 3D T2-FLAIR imaging would have been beneficial to improve segmentation accuracy for volumetry and electrode modelling.

In addition, normative connectivity is not reflective of patient-specific connectivity and may not capture disorder-related microstructural tract changes associated with cervical dystonia.(32,33)

Despite this, normative and patient-specific connectivity utility has been shown to be comparable in Parkinson's disease.(79)

Conclusions

Taken together, the results from this study support cervical dystonia as a network disorder and provide evidence for associations between the structure of key motor regions, and structural pathways with clinical motor outcomes. We show that dentate and brainstem nuclei morphometry may represent markers that determine the efficacy of DBS, outside of GPi targeting accuracy. Furthermore, we present the potential importance of the non-decussating DRTT in the pathophysiology and therapeutic targeting of cervical dystonia.

Acknowledgements: Mrs Bonnie O'Sullivan, Digital Systems PACS Manager at Radiology Directorate, The Walton Centre NHS Trust

Neurologists of Movement Disorders DBS Team, The Walton Centre NHS Trust: Dr Dinesh Damodaran, Dr Sundus Alusi, Dr Jay Panicker, Dr Michael Bonello

Ethical compliance statement:

This work was sponsored by the University of Liverpool and the Walton Centre NHS Trust. Approval for this work was obtained by HRA and Health and Care Research Wales (HRCW; REC reference number: 22/PR/1326).

Informed patient consent was not necessary for this work.

References

1. Crowner BE. Cervical Dystonia: Disease Profile and Clinical Management. Phys Ther. 2007 Nov 1;87(11):1511–26.

2. Krauss JK, Loher TJ, Pohle T, Weber S, Taub E, Bärlocher CB, et al. Pallidal deep brain stimulation in patients with cervical dystonia and severe cervical dyskinesias with cervical myelopathy. J Neurol Neurosurg Psychiatry. 2002 Feb;72(2):249–56.

3. Jacksch C, Zeuner KE, Helmers AK, Witt K, Deuschl G, Paschen S. Long-term efficacy with deep brain stimulation of the globus pallidus internus in cervical dystonia: a retrospective monocentric study. Neurol Res Pract. 2022 Oct 3;4(1):48.

4. Reich MM, Horn A, Lange F, Roothans J, Paschen S, Runge J, et al. Probabilistic mapping of the antidystonic effect of pallidal neurostimulation: a multicentre imaging study. Brain J Neurol. 2019 May 1;142(5):1386–98.

5. Okromelidze L, Tsuboi T, Eisinger RS, Burns MR, Charbel M, Rana M, et al. Functional and Structural Connectivity Patterns Associated with Clinical Outcomes in Deep Brain Stimulation of the Globus Pallidus Internus for Generalized Dystonia. AJNR Am J Neuroradiol. 2020 Mar;41(3):508–14.

6. Zittel S, Hidding U, Trumpfheller M, Baltzer VL, Gulberti A, Schaper M, et al. Pallidal lead placement in dystonia: leads of non-responders are contained within an anatomical range defined by responders. J Neurol. 2020 Jun;267(6):1663–71.

7. Prudente CN, Hess EJ, Jinnah HA. Dystonia as a network disorder: what is the role of the cerebellum? Neuroscience. 2014 Feb 28;260:23–35.

8. Kaji R, Bhatia K, Graybiel AM. Pathogenesis of dystonia: is it of cerebellar or basal ganglia origin? J Neurol Neurosurg Psychiatry. 2018 May;89(5):488–92.

9. LeDoux MS, Brady KA. Secondary cervical dystonia associated with structural lesions of the central nervous system. Mov Disord Off J Mov Disord Soc. 2003 Jan;18(1):60–9.

10. Corp DT, Joutsa J, Darby RR, Delnooz CCS, van de Warrenburg BPC, Cooke D, et al. Network localization of cervical dystonia based on causal brain lesions. Brain J Neurol. 2019 Jun 1;142(6):1660–74.

11. Corp DT, Greenwood CJ, Morrison-Ham J, Pullinen J, McDowall GM, Younger EFP, et al. Clinical and Structural Findings in Patients With Lesion-Induced Dystonia: Descriptive and Quantitative Analysis of Published Cases. Neurology. 2022 Nov 1;99(18):e1957–67.

12. Prudente CN, Pardo CA, Xiao J, Hanfelt J, Hess EJ, Ledoux MS, et al. Neuropathology of cervical dystonia. Exp Neurol. 2013 Mar;241:95–104.

13. Brüggemann N. Contemporary functional neuroanatomy and pathophysiology of dystonia. J Neural Transm Vienna Austria 1996. 2021 Apr;128(4):499–508.

14. Popa T, Hubsch C, James P, Richard A, Russo M, Pradeep S, et al. Abnormal cerebellar processing of the neck proprioceptive information drives dysfunctions in cervical dystonia. Sci Rep. 2018 Feb 2;8(1):2263.

15. Horn A, Reich MM, Ewert S, Li N, Al-Fatly B, Lange F, et al. Optimal deep brain stimulation sites and networks for cervical vs. generalized dystonia. Proc Natl Acad Sci U S A. 2022 Apr 5;119(14):e2114985119.

16. Dum RP, Strick PL. An unfolded map of the cerebellar dentate nucleus and its projections to the cerebral cortex. J Neurophysiol. 2003 Jan;89(1):634–9.

17. van den Brink RL, Pfeffer T, Donner TH. Brainstem Modulation of Large-Scale Intrinsic Cortical Activity Correlations. Front Hum Neurosci. 2019;13:340.

18. Basinger H, Hogg JP. Neuroanatomy, Brainstem. In: StatPearls [Internet]. Treasure Island (FL): StatPearls Publishing; 2022 [cited 2022 Oct 24]. Available from: http://www.ncbi.nlm.nih.gov/books/NBK544297/

19. Singh K, Cauzzo S, García-Gomar MG, Stauder M, Vanello N, Passino C, et al. Functional connectome of arousal and motor brainstem nuclei in living humans by 7 Tesla resting-state fMRI. NeuroImage. 2022 Apr 1;249:118865.

20. Carbon M, Kingsley PB, Tang C, Bressman S, Eidelberg D. Microstructural white matter changes in primary torsion dystonia. Mov Disord Off J Mov Disord Soc. 2008 Jan 30;23(2):234–9.

21. Blood AJ, Kuster JK, Woodman SC, Kirlic N, Makhlouf ML, Multhaupt-Buell TJ, et al. Evidence for altered basal ganglia-brainstem connections in cervical dystonia. PloS One. 2012;7(2):e31654.

22. Prell T, Peschel T, Köhler B, Bokemeyer MH, Dengler R, Günther A, et al. Structural brain abnormalities in cervical dystonia. BMC Neurosci. 2013 Oct 16;14:123.

23. Pontillo G, Castagna A, Vola EA, Macerollo A, Peluso S, Russo C, et al. The cerebellum in idiopathic cervical dystonia: A specific pattern of structural abnormalities? Parkinsonism Relat Disord. 2020 Nov;80:152–7.

24. Fečíková A, Jech R, Čejka V, Čapek V, Šťastná D, Štětkářová I, et al. Benefits of pallidal stimulation in dystonia are linked to cerebellar volume and cortical inhibition. Sci Rep. 2018 Nov 21;8(1):17218.

25. Prent N, Potters WV, Boon LI, Caan MWA, de Bie RMA, van den Munckhof P, et al. Distance to white matter tracts is associated with deep brain stimulation motor outcome in Parkinson's disease. J Neurosurg. 2019 Jul 26;1–10.

26. Dembek TA, Petry-Schmelzer JN, Reker P, Wirths J, Hamacher S, Steffen J, et al. PSA and VIM DBS efficiency in essential tremor depends on distance to the dentatorubrothalamic tract. NeuroImage Clin. 2020;26:102235.

27. Petry-Schmelzer JN, Dembek TA, Steffen JK, Jergas H, Dafsari HS, Fink GR, et al. Selecting the Most Effective DBS Contact in Essential Tremor Patients Based on Individual Tractography. Brain Sci. 2020 Dec 20;10(12):E1015.

28. Middlebrooks EH, Okromelidze L, Wong JK, Eisinger RS, Burns MR, Jain A, et al. Connectivity correlates to predict essential tremor deep brain stimulation outcome: Evidence for a common treatment pathway. NeuroImage Clin. 2021;32:102846.

29. Afifi AK, Bergman RA. Functional neuroanatomy: text and atlas. Vol. 10. McGraw-hill New York; 1998.

30. Meola A, Comert A, Yeh FC, Sivakanthan S, Fernandez-Miranda JC. The nondecussating pathway of the dentatorubrothalamic tract in humans: human connectome-based tractographic study and microdissection validation. J Neurosurg. 2016 May;124(5):1406–12.

31. Petersen KJ, Reid JA, Chakravorti S, Juttukonda MR, Franco G, Trujillo P, et al. Structural and functional connectivity of the nondecussating dentato-rubro-thalamic tract. NeuroImage. 2018 Aug 1;176:364–71.

32. Argyelan M, Carbon M, Niethammer M, Ulug AM, Voss HU, Bressman SB, et al. Cerebellothalamocortical connectivity regulates penetrance in dystonia. J Neurosci Off J Soc Neurosci. 2009 Aug 5;29(31):9740–7.

33. Sondergaard RE, Rockel CP, Cortese F, Jasaui Y, Pringsheim TM, Sarna JR, et al. Microstructural Abnormalities of the Dentatorubrothalamic Tract in Cervical Dystonia. Mov Disord Off J Mov Disord Soc. 2021 Sep;36(9):2192–8.

34. Consky E, Basinski A, Belle L, Ranawaya R, Lang A. The Toronto Western Spasmodic Torticollis Rating Scale (TWSTRS): assessment of validity and inter-rater reliability. Neurology. 1990;40(Suppl 1):445.

35. Loher TJ, Capelle HH, Kaelin-Lang A, Weber S, Weigel R, Burgunder JM, et al. Deep brain stimulation for dystonia: outcome at long-term follow-up. J Neurol. 2008 Jun;255(6):881–4.

36. Walsh RA, Sidiropoulos C, Lozano AM, Hodaie M, Poon YY, Fallis M, et al. Bilateral pallidal stimulation in cervical dystonia: blinded evidence of benefit beyond 5 years. Brain J Neurol. 2013 Mar;136(Pt 3):761–9.

37. Gonzalez-Escamilla G, Muthuraman M, Reich MM, Koirala N, Riedel C, Glaser M, et al. Cortical network fingerprints predict deep brain stimulation outcome in dystonia. Mov Disord Off J Mov Disord Soc. 2019 Oct;34(10):1537–46.

38. Kroneberg D, Plettig P, Schneider GH, Kühn AA. Motor Cortical Plasticity Relates to Symptom Severity and Clinical Benefit From Deep Brain Stimulation in Cervical Dystonia. Neuromodulation J Int Neuromodulation Soc. 2018 Dec;21(8):735–40.

39. Iglesias JE, Billot B, Balbastre Y, Tabari A, Conklin J, Gilberto González R, et al. Joint super-resolution and synthesis of 1 mm isotropic MP-RAGE volumes from clinical MRI exams with scans of different orientation, resolution and contrast. NeuroImage. 2021 Aug 15;237:118206.

40. Iglesias JE, Van Leemput K, Bhatt P, Casillas C, Dutt S, Schuff N, et al. Bayesian segmentation of brainstem structures in MRI. NeuroImage. 2015 Jun;113:184–95.

41. Diedrichsen J. A spatially unbiased atlas template of the human cerebellum. NeuroImage. 2006 Oct 15;33(1):127–38.

42. Ashburner J. A fast diffeomorphic image registration algorithm. NeuroImage. 2007 Oct 15;38(1):95–113.

43. Patenaude B, Smith SM, Kennedy DN, Jenkinson M. A Bayesian model of shape and appearance for subcortical brain segmentation. NeuroImage. 2011 Jun 1;56(3):907–22.

44. Horn A, Kühn AA. Lead-DBS: A toolbox for deep brain stimulation electrode localizations and visualizations. NeuroImage. 2015;107:127–35.

45. Horn A, Li N, Dembek TA, Kappel A, Boulay C, Ewert S, et al. Lead-DBS v2: Towards a comprehensive pipeline for deep brain stimulation imaging. NeuroImage. 2019 Jan 1;184:293–316.

46. Horn A, Reich M, Vorwerk J, Li N, Wenzel G, Fang Q, et al. Connectivity Predicts deep brain stimulation outcome in Parkinson disease. Ann Neurol. 2017 Jul;82(1):67–78.

47. Avants BB, Epstein CL, Grossman M, Gee JC. Symmetric diffeomorphic image registration with cross-correlation: evaluating automated labeling of elderly and neurodegenerative brain. Med Image Anal. 2008 Feb;12(1):26–41.

48. Fonov VS, Evans AC, McKinstry RC, Almli CR, Collins D. Unbiased nonlinear average age-appropriate brain templates from birth to adulthood. NeuroImage. 2009;(47):S102.

49. Setsompop K, Kimmlingen R, Eberlein E, Witzel T, Cohen-Adad J, McNab JA, et al. Pushing the limits of in vivo diffusion MRI for the Human Connectome Project. NeuroImage. 2013 Oct 15;80:220–33.

50. Ewert S, Plettig P, Li N, Chakravarty MM, Collins DL, Herrington TM, et al. Toward defining deep brain stimulation targets in MNI space: A subcortical atlas based on multimodal MRI, histology and structural connectivity. NeuroImage. 2018 Apr 15;170:271–82.

51. Middlebrooks EH, Domingo RA, Vivas-Buitrago T, Okromelidze L, Tsuboi T, Wong JK, et al. Neuroimaging Advances in Deep Brain Stimulation: Review of Indications, Anatomy, and Brain Connectomics. AJNR Am J Neuroradiol. 2020 Sep;41(9):1558–68.

52. Pintzka CWS, Hansen TI, Evensmoen HR, Håberg AK. Marked effects of intracranial volume correction methods on sex differences in neuroanatomical structures: a HUNT MRI study. Front Neurosci. 2015;9:238.

53. Treu S, Strange B, Oxenford S, Neumann WJ, Kuehn A, Li N, et al. Deep brain stimulation: Imaging on a group level. NEUROIMAGE. 2020 Oct 1;219.

54. Edlow BL, Mareyam A, Horn A, Polimeni JR, Witzel T, Tisdall MD, et al. 7 Tesla MRI of the ex vivo human brain at 100 micron resolution. Sci Data. 2019 Oct 30;6(1):244.

55. Palesi F, De Rinaldis A, Castellazzi G, Calamante F, Muhlert N, Chard D, et al. Contralateral cortico-ponto-cerebellar pathways reconstruction in humans in vivo: implications for reciprocal cerebro-cerebellar structural connectivity in motor and non-motor areas. Sci Rep. 2017 Oct 9;7(1):12841.

56. Haines DE, Mihailoff GA. Chapter 27 - The Cerebellum. In: Haines DE, Mihailoff GA, editors. Fundamental Neuroscience for Basic and Clinical Applications (Fifth Edition) [Internet]. Fifth Edition. Elsevier; 2018. p. 394-412.e1. Available from: https://www.sciencedirect.com/science/article/pii/B978032339632500027X

57. Park S, Jeong H, Chung YA, Kang I, Kim S, Song IU, et al. Changes of regional cerebral blood flow after deep brain stimulation in cervical dystonia. EJNMMI Res. 2022 Aug 9;12(1):47.

58. Loh A, Elias GJB, Germann J, Boutet A, Gwun D, Yamamoto K, et al. Neural Correlates of Optimal Deep Brain Stimulation for Cervical Dystonia. Ann Neurol. 2022 Sep;92(3):418–24.

59. Karnik V, Del Gamba C, Jesuthasan A, Latorre A. Cervical Dystonia Following Injury to the Cerebellar Pontine Angle: An Instructive Case. Mov Disord Clin Pract. 2018 Dec;5(6):659–60.

60. Shakkottai VG. Physiologic changes associated with cerebellar dystonia. Cerebellum Lond Engl. 2014 Oct;13(5):637–44.

61. Neychev VK, Fan X, Mitev VI, Hess EJ, Jinnah HA. The basal ganglia and cerebellum interact in the expression of dystonic movement. Brain J Neurol. 2008 Sep;131(Pt 9):2499–509.

62. Geminiani A, Mockevičius A, D'Angelo E, Casellato C. Cerebellum Involvement in Dystonia During Associative Motor Learning: Insights From a Data-Driven Spiking Network Model. Front Syst Neurosci. 2022;16:919761.

63. Kayakabe M, Kakizaki T, Kaneko R, Sasaki A, Nakazato Y, Shibasaki K, et al. Motor dysfunction in cerebellar Purkinje cell-specific vesicular GABA transporter knockout mice. Front Cell Neurosci. 2013;7:286.

64. Groth CL, Brown M, Honce JM, Shelton E, Sillau SH, Berman BD. Cervical Dystonia Is Associated With Aberrant Inhibitory Signaling Within the Thalamus. Front Neurol. 2020;11:575879.

65. White JJ, Sillitoe RV. Genetic silencing of olivocerebellar synapses causes dystonia-like behaviour in mice. Nat Commun. 2017 Apr 4;8:14912.

66. Aïssa HB, Sala RW, Georgescu Margarint EL, Frontera JL, Varani AP, Menardy F, et al. Functional abnormalities in the cerebello-thalamic pathways in a mouse model of DYT25 dystonia. eLife. 2022 Jun 14;11:e79135.

67. Baumgartner AJ, Thompson JA, Kern DS, Ojemann SG. Novel targets in deep brain stimulation for movement disorders. Neurosurg Rev. 2022 Aug;45(4):2593–613.

68. Nieuwenhuys R, Voogd J, van Huijzen C. The Human Central Nervous System: A Synopsis and Atlas. Springer Science & Business Media; 2013.

69. Sheridan N, Tadi P. Neuroanatomy, Thalamic Nuclei. In: StatPearls [Internet]. Treasure Island (FL): StatPearls Publishing; 2022 [cited 2022 Oct 26]. Available from: http://www.ncbi.nlm.nih.gov/books/NBK549908/

70. Delnooz CCS, Pasman JW, Beckmann CF, van de Warrenburg BPC. Task-free functional MRI in cervical dystonia reveals multi-network changes that partially normalize with botulinum toxin. PloS One. 2013;8(5):e62877.

71. Brodoehl S, Wagner F, Prell T, Klingner C, Witte OW, Günther A. Cause or effect: Altered brain and network activity in cervical dystonia is partially normalized by botulinum toxin treatment. NeuroImage Clin. 2019;22:101792.

72. Hok P, Hvizdošová L, Otruba P, Kaiserová M, Trnečková M, Tüdös Z, et al. Botulinum toxin injection changes resting state cerebellar connectivity in cervical dystonia. Sci Rep. 2021 Apr 15;11(1):8322.

73. Nambu A. Somatotopic Organization of the Primate Basal Ganglia. Front Neuroanat [Internet]. 2011 [cited 2023 Jan 11];5. Available from: http://journal.frontiersin.org/article/10.3389/fnana.2011.00026/abstract

74. Krauss JK, Yianni J, Loher TJ, Aziz TZ. Deep brain stimulation for dystonia. J Clin Neurophysiol Off Publ Am Electroencephalogr Soc. 2004 Feb;21(1):18–30.

75. Draganski B, Thun-Hohenstein C, Bogdahn U, Winkler J, May A. 'Motor circuit' gray matter changes in idiopathic cervical dystonia. Neurology. 2003 Nov 11;61(9):1228–31.

76. Bono F, Salvino D, Cerasa A, Vescio B, Nigro S, Quattrone A. Electrophysiological and structural MRI correlates of dystonic head rotation in drug-naïve patients with torticollis. Parkinsonism Relat Disord. 2015 Dec;21(12):1415–20.

77. Huang X, Zhang M, Li B, Shang H, Yang J. Structural and functional brain abnormalities in idiopathic cervical dystonia: A multimodal meta-analysis. Parkinsonism Relat Disord. 2022 Oct;103:153–65.

78. Zito GA, Tarrano C, Jegatheesan P, Ekmen A, Béranger B, Rebsamen M, et al. Somatotopy of cervical dystonia in motor-cerebellar networks: Evidence from resting state fMRI. Parkinsonism Relat Disord. 2022 Jan;94:30–6.

79. Wang Q, Akram H, Muthuraman M, Gonzalez-Escamilla G, Sheth SA, Oxenford S, et al. Normative vs. patient-specific brain connectivity in deep brain stimulation. NeuroImage. 2021 Jan 1;224:117307.